Spectrochimica Acta, Vol. 44A, No. 7, pp. 749–761, 1988.
Printed in Great Britain.

0584–8539/88 \$3.00+0.00

Vibrational spectra and normal coordinate analysis of *p*-cresol and its deuterated analogs

HIDEO TAKEUCHI, NORIKO WATANABE and ISSEI HARADA
Pharmaceutical Institute, Tohoku University, Aobayama, Sendai 980, Japan

(*Received* 6 *October* 1987; *accepted* 24 *November* 1987)

Abstract—I.r. and Raman spectra of *p*-cresol and its seven deuterated analogs were investigated in dilute solutions of hydrophobic solvents. Assignments of the observed i.r. and Raman bands were made on the basis of isotopic frequency shifts, Raman polarization properties, i.r. intensities and normal coordinate calculations. The calculated normal frequencies are in good agreement with the experimental ones: the average error below 1700 cm^{-1} is 3.8 cm^{-1} for 164 in-plane vibrations and 3.3 cm^{-1} for 59 out-of-plane vibrations. The calculated vibrational modes may be useful in analysing the vibrational spectra of tyrosine. It is suggested that several doublets due to Fermi resonance and a trio of Raman bands in the 1260–1160 cm^{-1} region are potential probes for the micro-environments of tyrosine side chains in proteins.

INTRODUCTION

Raman spectra of proteins give information on the structure of the main chain and the micro-environments of side chains in the proteins [1]. Tryptophan, tyrosine and phenylalanine are particularly important amino acid residues in the Raman spectroscopic studies of protein structure, because the side chain vibrations of these aromatic residues are strong in the Raman spectra of vis.-light excitation and, furthermore, they can be selectively enhanced by u.v.-light excitation [1–6]. Interpretation of the Raman spectra of proteins, therefore, requires the knowledge of vibrational modes characteristic of the aromatic side chains. We have studied the vibrational modes of the tryptophan side chain in previous work [7] and here we extend the work to the tyrosine side chain.

The simplest model of the tyrosine side chain is *p*-cresol (4-methylphenol). JACKOBSEN reported Raman spectra of this compound and its three deuterated derivatives in the liquid state and the i.r. spectra in the liquid, solution, vapor and solid states [8]. DAVYDOVA *et al.* calculated the normal frequencies of out-of-plane vibrations and assigned some of the infrared and Raman bands [9]. GREEN *et al.* proposed complete assignments of fundamental frequencies for non-deuterated *p*-cresol [10].

In this study, we have measured infrared and Raman spectra of eight isotopomers of *p*-cresol (d_0, d_0-OD, 2,6-d_2, 2,6-d_2-OD, 3,5-d_2, 3,5-d_2-OD, 2,3,5,6-d_4 and 2,3,5,6-d_4-OD) in dilute solutions of non-polar solvents. The observed i.r. and Raman bands have been assigned on the basis of isotopic frequency shifts, Raman polarization properties and i.r. intensities. Using the experimental frequencies, a molecular force field has been obtained, which reproduces experimental data satisfactorily and confirms the assignments.

EXPERIMENTAL

Reagent grade *p*-cresol was obtained commercially and used without further purification. Deuteration in the benzene ring was performed by acid-catalyzed exchange reactions [8, 11, 12]. (i) *p*-Cresol-2,6-d_2-OD was prepared by refluxing 1 g of *p*-cresol with 4 ml of D_2O (> 99.8%, D) and 0.2 ml of concentrated D_2SO_4 (> 99%, D) at 100–120°C for 20 h. The product was extracted with petroleum ether and the solvent was removed from the extract on a rotary evaporator. The residue was then dissolved in petroleum ether and kept at −20°C for several hours during which time the product crystallized out. The crystallization procedure was repeated until the product was obtained as colorless needles and non-fluorescent in the Raman measurements. (ii) The preparation of *p*-cresol-2,3,5,6-d_4-OD followed a procedure similar to (i) except that the amount of D_2SO_4 used was 1 ml and the reflux was repeated twice at 150°C. (iii) *p*-Cresol-3,5-d_2-OH was prepared from the 2,3,5,6-d_4-OD compound by a method parallel to (i) using H_2O and H_2SO_4 instead of D_2O and D_2SO_4. NMR spectra showed that the isotopic purity was better than 90% for all the deuterated compounds (the proton NMR signals were observed at 6.8 ppm for the 2 and 6 positions and at 7.1 ppm for the 3 and 5 positions in D_2O solution containing sodium 2,2-dimethyl-2-silapentane-5-sulfate as the internal standard). H–D exchange of the hydroxyl group was made by dissolving the sample in a hydrophobic solvent (CS_2, $CCl_2=CCl_2$ or cyclopentane) and then washing the solution with H_2O or D_2O.

I.r. spectra of the eight isotopomers of *p*-cresol between 4000 and 400 cm^{-1} were recorded on a JASCO IR-810 i.r. spectrophotometer with a KBr cell of 1 mm thickness using the solvents $CCl_2=CCl_2$ (4000–1400 cm^{-1} and 600–400 cm^{-1}) and CS_2 (1400–600 cm^{-1}). The sample concentration was 50 mM and the self-association was negligible. The solvent absorption was subtracted from the solution spectra. The wavenumber axis was calibrated using liquid indene and gaseous H_2O, CO_2, CO and HCl.

Raman spectra were excited with 488 nm light of an Ar ion laser and recorded on a JASCO 80D double monochromater equipped with a multichannel detection system (SMA, Princeton Instruments). The solvents used were CS_2 (3100–2200 cm^{-1} and 1650–850 cm^{-1}) and cyclopentane (850–300 cm^{-1}) with a sample concentration of 100 mM. The spectra of solvents were measured separately and subtracted from the solution spectra. Polarization measurements were also made. The wavenumber axis was calibrated for indene.

NORMAL COORDINATE CALCULATIONS

Calculations of normal frequencies and modes as well as the least squares refinements of force constants were made by use of the computer program NCTB [13] based on the *GF* matrix method.

The geometrical parameters used in the normal coordinate calculations are listed in Table 1 and the atom numbering scheme is shown in Fig. 1. The C–C and C–O bond lengths and the CCC and CCO angles were calculated from the X-ray crystallographic data on *p*-cresol [14] by assuming C_{2v} symmetry of the molecular skeleton. The orientations of the OH and CH_3 groups were also taken from the crystallographic data, which showed that the OH hydrogen atom and one of the CH_3 hydrogen atoms lay in the plane of the benzene nucleus. The O–H length and COH angle were taken from the microwave data on phenol [15]. The ring C–H bonds were assumed to be 1.084 Å in length and to bisect the CCC angle. For the CH_3 group, a geometry with C_{3v} local symmetry was adopted, which had been used in normal coordinate calculations on aliphatic hydrocarbons [13]. The structure of *p*-cresol assumed here has a plane of symmetry.

Internal coordinates are defined following the IUPAC recommendations [6]. The coordinates consist of 16 stretches (7νCH, νOH, 6νCC, νCCH_3 and νCO), 25 bends (11ϕCCH, 3ϕHCH, ϕCOH, 6ϕCCC, 2$\phi CCCH_3$ and 2ϕCCO), six out-of-plane waggings (4πCH, πCCH_3 and πCO) and eight torsions (6τCC, τCCH_3 and τCO). The displacements of the *X* atoms of all πCX are the same in direction. Each torsional coordinate involves all the atoms attached to the torsional axis.

The potential energy is expressed in terms of the basis coordinates, most of which are internal coordinates themselves and the others are linear combinations of internal coordinates. The linear combinations are so chosen that the basis coordinates are symmetric (in-plane) or antisymmetric (out-of-plane) with respect to the plane of symmetry and that the number of redundancies is reduced. Six in-plane redundancies are eliminated by defining the following combinations of bending coordinates.

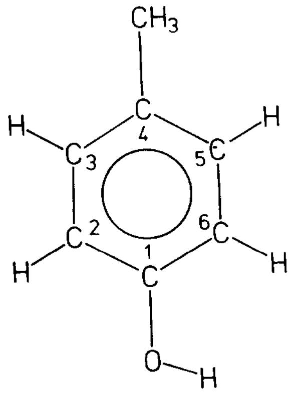

Fig. 1. Atom numbering scheme for *p*-cresol.

$$\delta C_jX = (\phi C_iC_jX - \phi C_kC_jX)/2^{1/2} \tag{1}$$

$$\gamma C_iC_jC_k = (2\phi C_iC_jC_k - \phi C_iC_jX - \phi C_kC_jX)/6^{1/2}. \tag{2}$$

Here *X* is H, CH_3 or O; *i*, *j* and *k* are atom indices; all δC_jX result in displacements of the *X* atoms in the same direction. For the CH_3 group vibrations, eight local symmetry coordinates, which are the same as those given in Ref. [13], are taken as the basis coordinates and one redundancy is eliminated. The other redundancies, which arise from ring constraints on the skeletal stretching, bending and torsional coordinates, are not eliminated explicitly and six zero-frequency modes corresponding to the redundancy coordinates (three for each of the in-plane and out-of-plane species) are obtained in the process of *GF* matrix diagonalization.

Initial values of force constants were taken from alkyl benzenes [17] and indole [7] for the benzene ring, from aliphatic hydrocarbons [13] for the CH_3 group and from ethylene glycol [18] for the COH group. Since the barrier to the CH_3 torsion in toluene is known to be very low [19] and the fundamental frequency of the CH_3 torsion in *p*-cresol is unknown,

Table 1. Geometrical parameters of *p*-cresol used in the normal coordinate calculations

Bond length (Å)		Bond angle (°)	
C_1–C_2, C_1–C_6	1.388	$C_1C_2C_3$, $C_1C_6C_5$	119.3
C_2–C_3, C_5–C_6	1.398	$C_2C_3C_4$, $C_4C_5C_6$	121.4
C_3–C_4, C_4–C_5	1.398	$C_2C_1C_6$	120.7
C_1–O	1.391	$C_3C_4C_5$	117.9
C_4–CH_3	1.517	$C_3C_4CH_3$	121.1
C–H (ring)	1.084	C_2C_1O	119.7
C–H (methyl)	1.100	C_1C_2H, C_1C_6H	120.4
O–H	0.956	C_4C_3H, C_4C_5H	119.3
		C_4CH (methyl)	110.4
		C_1OH	109.0

we assumed a small value, 0.0005 mdynÅ rad^{-2}, as the CH_3 torsional force constant in order to avoid coupling between the CH_3 torsion and the other vibrations. Refinements of the force constants were made by the least squares fitting of the calculated frequencies to the experimental ones.

The experimental frequencies of fundamentals were selected from the i.r. and Raman data observed in this work. Exceptions were several frequencies below 330 cm^{-1}, which were taken from Refs [8] and [10]. For doublet bands due to Fermi resonance, intensity-weighted mean frequencies were used as the fundamental frequencies.

RESULTS AND DISCUSSION

I.r. spectra of *p*-cresol and its deuterated analogs in the 4000–2000 cm^{-1} region are shown in Fig. 2. The O–H and O–D stretching bands appear at 3611 and 2668 cm^{-1}, respectively. Assignment of the C–H stretching vibrations of the ring and the methyl group is not straightforward because of many possibilities of overlap and Fermi resonance with combinations and overtones. For the ring C–H stretching modes, the strongest i.r. and Raman bands in the 3100–3000 cm^{-1} region are tentatively chosen as fundamentals (the Raman bands are polarized). Their frequencies are 3028 cm^{-1} (i.r.) and 3057 cm^{-1} (Raman) for *p*-cresol-d_0 and 3027 cm^{-1} (i.r. and Raman) for the 2,6-d_2 and 3,5-d_2 compounds. Similarly the fundamental frequencies of the C–D stretching vibrations are selected: the average (2263 cm^{-1}) of 2253 cm^{-1} (i.r.) and 2273 cm^{-1} (Raman) for 2,6-d_2; 2256 cm^{-1} (i.r. and Raman) for 3,5-d_2; 2260 cm^{-1} (i.r.) and 2264 cm^{-1} (Raman) for 2,3,5,6-d_4. The symmetric C–H stretching vibration of the CH_3 group is assigned to the 2920 cm^{-1} i.r. band, the corresponding Raman band being strong and polarized. The degenerate C–H stretching vibration is assigned to a shoulder at 2945 cm^{-1}, which is observed in the i.r. spectra of all the compounds studied here. An i.r. absorption and a polarized Raman band are observed around 2865 cm^{-1} and attributable to the first overtone of the CH_3 degenerate bending vibration as in the case of toluene [20]. In the normal coordinate calculations, only the C–H and O–H stretching frequencies are used for the refinement of force constants because of significant difference in anharmonicity between the C–H (O–H) and C–D (O–D) stretching vibrations.

Figures 3–6 show the i.r. and Raman spectra below 1650 cm^{-1}. The spectra recorded in different solvents and in different wavenumber regions are merged into a spectrum for each compound by using the bands in the

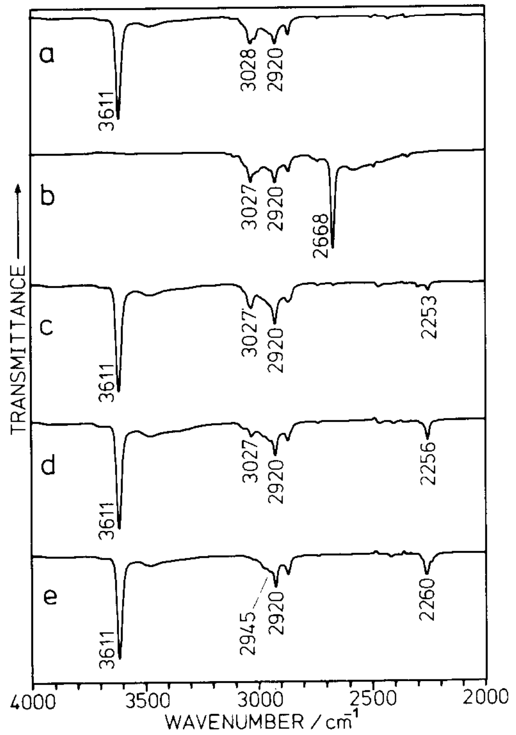

Fig. 2. Infrared spectra of *p*-cresol between 4000 and 2000 cm^{-1} in $CCl_2{=}CCl_2$ solution (50 mM): (a) *p*-cresol-d_0; (b) *p*-cresol-d_0-OD; (c) *p*-cresol-2,6-d_2; (d) *p*-cresol-3,5-d_2; (e) *p*-cresol-2,3,5,6-d_4.

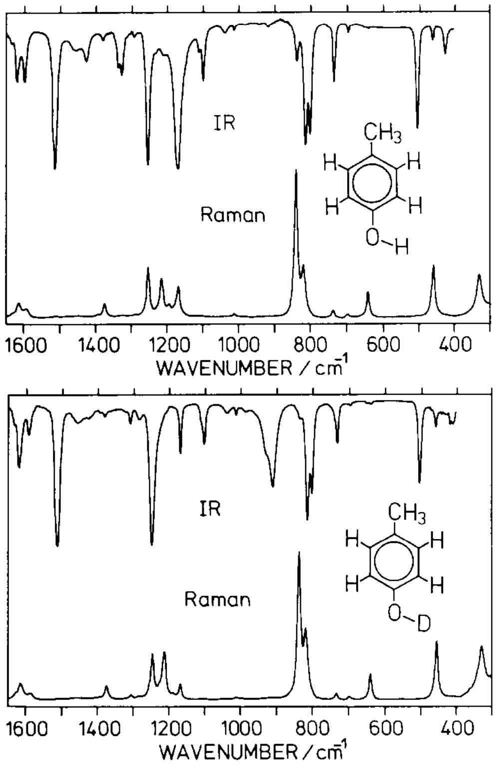

Fig. 3. I.r. and Raman spectra of *p*-cresol-d_0 and its OD compound. I.r. spectra: the 1650–1400 and 600–400 cm^{-1} regions in $CCl_2{=}CCl_2$ and the 1400–600 cm^{-1} region in CS_2 with a concentration of 50 mM. Raman spectra: the 1650–850 cm^{-1} region in CS_2 and the 850–300 cm^{-1} region in cyclopentane with a concentration of 100 mM.

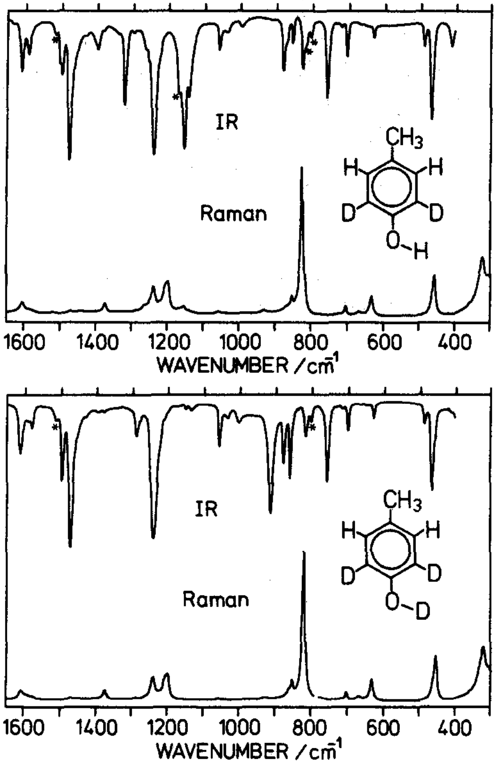

Fig. 4. I.r. and Raman spectra of *p*-cresol-2,6-d_2 and its OD compound. Solvents and concentrations are the same as in Fig. 3. The bands marked with * are due to *p*-cresol-d_0.

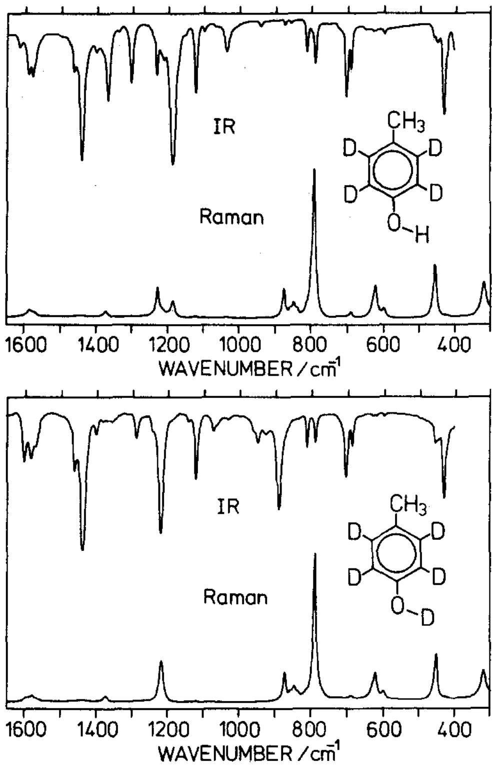

Fig. 6. I.r. and Raman spectra of *p*-cresol-2,3,5,6-d_4 and its OD compound. Solvents and concentrations are the same as in Fig. 3.

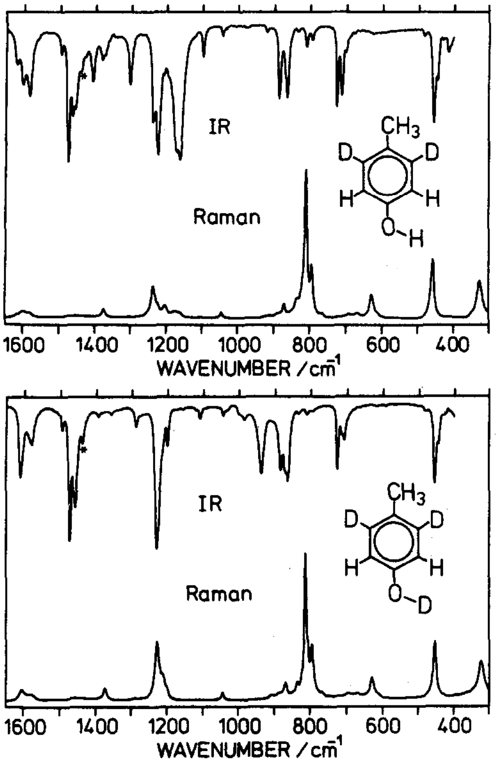

Fig. 5. I.r. and Raman spectra of *p*-cresol-3,5-d_2 and its OD compound. Solvents and concentrations are the same as in Fig. 3. The bands marked with * are due to *p*-cresol-2,3,5,6-d_4.

overlapping wavenumber region as the intensity standard. Most of the bands observed in the spectra are assigned to fundamentals, though some bands are attributed to combinations or overtones. Isotopic frequency shifts, Raman polarization properties and i.r. intensities are useful in making the assignments. From the frequency shifts on deuteration at the hydroxyl group, a strong i.r. band in the 1190–1150 cm^{-1} region is assigned to ϕCOH and that in the 950–890 cm^{-1} region to ϕCOD. The other bands that shift on deuteration of the hydroxyl group are ascribed to in-plane modes because such bands must be more or less contributed from ϕCOH or ϕCOD. Another mode sensitive to the OH → OD substitution is τCO. However, this out-of-plane mode has a frequency of 290 cm^{-1} [8] and its deuteration shift would not significantly affect the vibrations above 300 cm^{-1}, the wavenumber region of the present measurements. Deuteration in the benzene ring is also helpful to the assignment. Vibrations characteristic of the CH_3 group are identified by their relative insensitiveness to the deuteration. Discrimination of C–H bend and C–H wagging modes from skeletal modes can be made by the deuteration shifts. Raman polarization properties and infrared intensities give information on the symmetry of vibration. If the vibration of the benzene ring does not strongly couple with those of the substituents, the benzene ring vibrations are classified under C_{2v} symmetry into A_1, A_2,

B_1 and B_2 species, the A_1 and B_2 modes being in-plane and the A_2 and B_1 modes out-of-plane. All the modes are Raman active and all but the A_2 modes are i.r. active. Only the Raman band due to the A_1 modes are polarized. According to these predictions based on the assumption of effective C_{2v} symmetry, polarized Raman bands are assigned to A_1 modes and infrared bands with high to medium intensities are assigned to A_1, B_1 or B_2 but not to A_2 modes. The assignments made in the manner described above are consistent with the results of normal coordinate calculations.

The force constants used in the normal coordinate calculations are listed in Table 2. The calculated fundamental frequencies below 1700 cm^{-1} are compared with the experimental ones in Table 3. The average deviation of the calculated frequencies from experimental ones is 3.8 cm^{-1} for 164 in-plane fundamentals and 3.3 cm^{-1} for 59 out-of-plane ones. Approximate descriptions of the calculated vibrational modes are also given in Table 3. For the vibrations characteristic of *p*-disubstituted benzene, notations of the corresponding vibrations in benzene [21] are

Table 2. Force constants

No.	Coordinates involved	Value*	Error†
Stretch			
1	νCH (ring)	4.9986	0.0052
2	νCC (ring)	6.8376	0.2593
3	νCCH$_3$	4.8537	0.1744
4	νCO	5.5082	0.2266
5	CH$_3$ symmetric stretch	4.8958	0.0072
6	CH$_3$ degenerate stretch	4.6145	0.0048
7	νOH	7.2755	0.0122
Bend			
8	δCH	0.5037	0.0028
9	δCCH$_3$	0.9243	0.0511
10	δCO	1.0242	0.0549
11	γCCC	0.7835	0.0368
12	CH$_3$ symmetric deformation	0.5766	0.0105
13	CH$_3$ degenerate deformation	0.5302	0.0134
14	CH$_3$ rock	0.7092	0.0179
15	φCOH	0.7640	0.0102
Stretch–stretch			
16	νCH/νCH (*ortho*)	0.0477	0.0072
17	νCC/νCC (*ortho*)	0.8339	0.1109
18	νCC/νCC (*meta*)	−0.3992	0.1706
19	νCC/νCC (*para*)	0.4163	0.1231
20	νCCH$_3$/νCC, νCO/νCC (C common)	0.1949	0.0392
21	νCCH$_3$/νCO	−0.0823	0.1765
Stretch–bend			
22	νCC/δCH (C common)‡	0.1353	0.0087
23	νCC/δCCH$_3$, νCC/δCO (C common)‡	0.2638	0.0230
24	νCC/γCCC (CC common)	0.3323	0.1249
25	νCCH$_3$/γCCC, νCO/γCCC (central C common)	−0.5531	0.0284
26	νCCH$_3$/CH$_3$ symmetric deformation	−0.3991	0.0628
27	νCO/δCOH	0.3883	0.0399
Bend–bend			
28	δCH/δCH (*ortho*)	0.0070	0.0029
29	δCH/δCH (*meta*)	−0.0136	0.0028
30	δCH/δCH (*para*)	0.0040	0.0027
31	γCCC/γCCC (CC common)	−0.0528	0.0215
32	δCH/γCCC (terminal C common)	0.0115	0.0089
33	CH$_3$ degenerate deformation/CH$_3$ rock	0.0267	0.0159
34	δCCH$_3$/γCCC, δCO/γCCC (terminal C common)	0.0518	0.0224
35	δCCH$_3$/δCO	−0.1036	0.0314
36	δCO/φCOH	0.0541	0.0188
Wagging			
37	πCH	0.4955	0.0293
38	πCCH$_3$	0.4430	0.0557
39	πCO	0.4971	0.0365
Torsion			
40	τCC	0.2244	0.0790
41	τCO	0.0397	0.0025
42	τCCH$_3$	0.0005	

Table 2. (*Contd.*)

No.	Coordinates involved	Value*	Error†
Wagging–wagging			
43	πCH/πCH (*ortho*)	0.0076	0.0228
44	πCH/πCH (*meta*)	−0.0368	0.0239
45	πCH/πCH (*para*)	−0.0364	0.0092
46	πCH/πCCH$_3$, πCH/πCO (*ortho*)	0.0582	0.0241
47	πCH/πCCH$_3$, πCH/πCO (*meta*)	−0.0664	0.0198
48	πCCH$_3$/πCO	−0.0036	0.1112
Wagging–torsion			
49	πCH/τCC (C common)§	−0.0785	0.0122
50	πCCH$_3$/τCC, πCO/τCC (C common)§	−0.0088	0.0365
51	πCH/τCC, πCCH$_3$/τCC, πCO/τCC (C uncommon)‖	−0.0432	0.0658
52	πCO/τCO¶	0.0227	0.0208
Torsion–torsion			
53	τCC/τCC (C common)	−0.0814	0.0784

*Units are mdynÅ^{-1} for stretch and stretch–stretch interaction constants, mdyn (rad)$^{-1}$ for stretch–bend constants and mdynÅ (rad)$^{-2}$ for the others.

†Standard errors obtained in the least squares refinement of the force constants. The constant for the methyl torsion was fixed.

‡When X of δCX (X = H, O or CH$_3$) moves toward the C–C bond of νCC, this constant is multiplied by −1.

§This constant represents an interaction where X of πCX (X = H, O or CH$_3$) moves in the same direction as in the torsional motion. When the directions are opposite to each other, the sign is reversed.

‖This constant applies to the case where the central carbon atom of the wagging coordinate moves in the same direction as in the torsion. When the directions are opposite to each other, the sign is reversed.

¶The direction of movement of the oxygen atom in πCO is the same as that of the hydrogen atom in τCO.

given together with the symmetry species under C_{2v} symmetry. The notations of benzene vibrations will be used to name the normal vibrations of *p*-cresol, though the correspondence is not always good for the vibrations of the partially deuterated ring. Figures 7 and 8 illustrate the normal modes of *p*-cresol-d_0 except for the CH$_3$ group vibrations.

The 842–823 cm^{-1} doublet in the Raman spectrum of *p*-cresol-d_0 has been ascribed to Fermi resonance between the ring-breathing vibration, $\nu_1(A_1)$, and the overtone of an out-of-plane ring-bending vibration, $\nu_{16a}(A_2)$ [22]. The corresponding doublet in tyrosine is called the 'tyrosine doublet' and is useful in the Raman spectroscopic characterization of tyrosine side chains in proteins because the intensity ratio of the doublet is sensitive to the state of hydrogen bonding or the ionization of the phenolic hydroxyl group [22]. On deuteration in the benzene ring, ν_{16a} shifts down greatly compared to ν_1 and the separation between ν_1 and $2\nu_{16a}$ becomes too large to cause the resonance interaction between the two energy levels effectively (the $2\nu_{16a}$ band is observed as a very weak Raman band at 776 cm^{-1} for *p*-cresol-2,6-d_2, at 770 cm^{-1} for *p*-cresol-3,5-d_2 and at 726 cm^{-1} for *p*-cresol-2,3,5,6-d_4). The removal of the Fermi resonance results in the appearance of a singlet ν_1 band at 828 cm^{-1} for *p*-cresol-2,6-d_2 and at 793 cm^{-1} for *p*-cresol-2,3,5,6-d_4. On the other hand, the ν_1 band is observed as a doublet at 815–799 cm^{-1} for *p*-cresol-3,5-d_2. The origin of this doublet may be ascribed to Fermi resonance between ν_1 and a combination, ν_4 (B_1, 670 cm^{-1}, Raman) + ν_{17b}(B_1, 143 cm^{-1}, calcd.).

A ring CC stretching mode (ν_{8a}) also undergoes Fermi resonance in two isotopomers and is observed as a doublet at 1618–1602 cm^{-1} for *p*-cresol-3,5-d_2 and at 1600–1582 cm^{-1} for *p*-cresol-2,3,5,6-d_4-OD. A characteristic of these doublets is that they become singlets on H–D exchange at the hydroxyl group. Since the ν_{8a} frequency is insensitive to the H–D exchange, the combination or overtone taking part in the Fermi resonance must involve at least one vibration whose frequency is sensitive to the H–D exchange, namely one of ν_{19b}, ν_{14}, ν_{7a}, ν_3, ν_{9b}, ϕCOH (ϕCOD), τCO and CH$_3$ in-plane rock weakly coupled with ϕCOH. The first and second overtones of these vibrations are far apart from ν_{8a} and unlikely to be the origin of the Fermi doublet. A possible combination interacting with ν_{8a} (A_1) is ν_{14} (B_2) + ν_{18b} (B_2), the sum of frequencies being 1303 + 330 = 1633 cm^{-1} for *p*-cresol-3,5-d_2 and 1287 + 323 = 1610 cm^{-1} for *p*-cresol-2,3,5,6-d_4-OD. The corresponding combination is observed as a weak i.r. band at 1632 cm^{-1} for *p*-cresol-2,6-d_2 and at 1612 cm^{-1} for *p*-cresol-2,3,5,6-d_4(the sums of frequencies are 1644 and 1622 cm^{-1}, respectively).

The doublet at 1335 and 1326 cm^{-1} in the i.r.

spectrum of *p*-cresol-d_0 is ascribed to Fermi resonance between $\nu_3(B_2)$ and, probably, a combination of out-of-plane modes, $\nu_{10a}(A_2, 831\ \mathrm{cm}^{-1}$, calcd.) + $\nu_{16b}(B_1$, 504 cm^{-1}, i.r. and Raman) or ν_5 (B_1, 920 cm^{-1}, i.r.) + $\nu_{16a}(A_2, 414\ \mathrm{cm}^{-1}$, Raman). The ν_3 mode shifts down to 1307 cm^{-1} on deuteration of the hydroxyl group, while the combination does not shift. Thus the Fermi resonance no longer takes place.

A C–H out-of-plane wagging mode, $\nu_{11}(B_1)$, appears as a doublet at 817–804 cm^{-1} in the i.r. spectra of CS_2 solutions of *p*-cresol-d_0 and its OD compound. In the liquid state the doublet disappears and a singlet band is observed at 814 cm^{-1}. Since the ν_{11} mode is observed as a strong singlet in the i.r. spectra of ring-deuterated compounds, the doublet of undeuterated *p*-cresol must be due to Fermi resonance. A combination possible to interact with ν_{11} is $2\nu_{18b}+\nu_{17b}$, where ν_{18b} and ν_{17b} belong to the B_2 and B_1 species, respectively, and the combination frequency is estimated as $2\times 334+144=812$ cm^{-1} for *p*-cresol-d_0 and $2\times 333+140=806$ cm^{-1} for *p*-cresol-d_0-OD.

In addition to the i.r. and Raman bands listed in Table 3 and discussed above, the spectra show some i.r. and Raman bands, which can be attributed to combinations or overtones. However, the unique assignment of these bands is difficult because a number of combinations and overtones are expected in the 1700–300 cm^{-1} region, particularly above 1000 cm^{-1}. Tentative assignments of combination and overtone bands are listed in Table 4.

p-Substituted phenol ring in tyrosine shows i.r. and Raman spectra very similar to those of *p*-cresol and the assignments described above for *p*-cresol can be transferred to tyrosine. The results of the present study are, therefore, expected to be useful in interpreting the vibrational spectra of tyrosine and deuterated tyrosine side chains in proteins. Incorporation of deuterated tyrosine in a protein has recently been demonstrated

Table 3. Fundamental frequencies of *p*-cresol and its deuterated compounds

d_0		d_0-OD		
ν_{obs}*	ν_{calc}	ν_{obs}*	ν_{calc}	Assignment†
In-plane				
1618 m, 9p	1621	1618 m, 10p	1620	νCC, 8a, A_1
1597 *m*, 5dp	1604	1591 m, 4dp	1596	νCC, 8b, B_2
1514 vs, 0	1521	1513 vs, 0	1519	νCC + δCH, 19a, A_1
1455 w, 0	1465	1457 w, 0	1461	CH_3 deg. deform.
1425 m, —	1425	1416 w, —	1413	νCC + δCH, 19b, B_2
1378 w, 8p	1378	1378 w, 9p	1378	CH_3 sym. deform.
1335 m, 0 ‡ 1326 m, 0 ‡	1331	1307 w, 2dp	1308	δCH + νCC, 3, B_2
1291 w, 0	1298	1281 w, 0	1291	νCC + δCH, 14, B_2
1254 vs, 32p	1249	1248 vs, 29p	1246	νCO, 7a′, A_1
1217 —, 25p	1214	1215 —, 32p	1212	νCCH_3, 7a, A_1
1170 —, 20p	1168	1169 m, 10p	1170	δCH, 9a, A_1
1169 vs, —	1173	913 s, —	915	ϕCOH (ϕCOD)
1100 m, —	1100	1102 m, 0	1105	δCH, 15, B_2
1014 w, 2p	1020	1014 w, 1p	1020	νCC + γCCC, 18a, A_1
984 vw, —	981	987 w, —	985	CH_3 rock
842 m, 100p ‡ 823 —, 35p ‡	830	839 w, 100p ‡ 821 —, 48p ‡	829	νCCH_3 + νCO, + νCC, 1, A_1
739 m, 5p	743	735 m, 4p	736	νCCH_3 + νCO, 13, A_1
645 vw, 17dp	649	644 vw, 17dp	649	γCCC, 6b, B_2
461 w, 34p	459	457 w, 38p	456	γCCC, 6a, A_1
422 m, —	427	407 w, —	411	δCO + δCCH_3, 9b, B_2
334 —, 23dp	332	333 —, 24dp	327	δCCH_3 + δCO, 18b, B_2
Out-of-plane				
1455 w, 0	1458	1457 w, 0	1458	CH_3 deg. deform.
1039 w, —	1040	1039 w, —	1040	CH_3 rock
948 vw, —	956	—	956	πCH, 17a, A_2
920 w, —	927	—	927	πCH, 5, B_1
	831	—	831	πCH, 10a, A_2
817 s, — ‡ 804 s, — ‡	817	817 s, — ‡ 804 s, — ‡	817	πCH, 11, B_1
700 w, 3dp	698	700 vw, 2dp	698	πCO + πCCH_3 + πCH, 4, B_1
504 s, 0	503	504 s, —	503	πCO + πCCH_3, 16b, B_1
414 —, 0§	426	416 w, —	425	τCC, 16a, A_2
320‖	313	—	312	πCCH_3 + πCO + τCC, 10b, B_1
294¶	293	—	219	τCO
—	144	—	140	τCC + πCCH_3 + πCO, 17b, B_1
—	17	—	17	τCCH_3

Table 3. (*Contd.*)

2,6-d_2		2,6-d_2-OD		
ν_{obs}*	ν_{calc}	ν_{obs}*	ν_{calc}	Assignment†
In-plane				
1607 m, 7p	1609	1611 m, 6p	1608	νCC, 8a, A_1
1588 m, 3dp	1588	1580 w, 2dp	1580	νCC, 8b, B_2
1474 vs, 2	1478	1472 vs, 1p	1474	νCC + δCH, 19a, A_1
1453 —, 0	1460	1448 —, 0	1458	CH$_3$ deg. deform.
1396 m, —	1398	—	1385	νCC + δCH, 19b, B_2
1378 vw, 6p	1378	1377 vw, 6p	1378	CH$_3$ sym. deform.
1319 s, 0	1325	1287 m, 0	1294	νCC + δCH, 14, B_2
1252 sh, —	1247	1222 sh, —	1224	νCC + δCH, 3, B_2
1240 vs, 14p	1232	1241 vs, 15p	1239	νCO, 7a′, A_1
1202, —, 18p	1200	1202 —, 16p	1200	νCCH$_3$, 7a, A_1
1154 vs, 4p	1147	917 s, 0	914	ϕCOH (ϕCOD)
1058 m, 1p	1056	1058 m, 1p	1056	δCH + δCD, 9a, A_1
996 w, —	995	1003 w, —	1000	CH$_3$ rock
872 sh, 0	873	863 m, —	871	δCD, 15, B_2
855 m, 5p	862	855 —, 8p	858	δCD, 18a, A_1
828 m, 100p	818	822 m, 100p	815	νCCH$_3$ + νCO + νCC, 1, A_1
706 m, 5p	710	704 m, 5p	705	νCCH$_3$ + νCO, 13, A_1
636 —, 12dp	637	635 —, 14dp	637	γCCC, 6b, B_2
460 —, 26p	458	456 sh, 29p	454	γCCC, 6a, A_1
407 m, —	414	—	399	δCO + δCCH$_3$, 9b, B_2
325 —, 24dp	331	325 —, 25 dp	325	δCCH$_3$ + δCO, 18b, B_2
Out-of-plane				
—	1458	—	1458	CH$_3$ deg. deform.
1036 w, 0	1039	1036 w, —	1039	CH$_3$ rock
914 vw, —	912	—	912	πCH, 17a, A_2
881 m, —	876	881 m, —	876	πCH, 5, B_1
758 s, —	760	758 s, —	760	πCD + πCO, 11, B_1
721 vw, —	712	718 vw, —	712	πCD, 10a, A_2
631 w, —	634	631 w, —	634	πCCH$_3$ + τCC, 4, B_1
463 s, —	467	462 s, —	466	πCO + πCCH$_3$, 16b, B_1
388 —, 0§	387	—	387	τCC, 16a, A_2
—	306	—	304	πCCH$_3$ + πCO + τCC, 10b, B_1
291¶	292	—	218	τCO
—	143	—	139	τCC + πCCH$_3$ + πCO, 17b, B_1
—	17	—	17	τCCH$_3$

Table 3. (*Contd.*)

3,5-d_2		3,5-d_2-OD		
ν_{obs}*	ν_{calc}	ν_{obs}*	ν_{calc}	Assignment†
In-plane				
1618 w, 0 1602 m, 4p ‡	1610	1610 m, 7p	1608	νCC, 8a, A_1
1584 m, 3dp	1591	1580 m, 3dp	1583	νCC, 8b, B_2
1475 vs, 0	1481	1474 vs, —	1478	νCC + δCH, 19a, A_1
1462 m, —	1461	1459 s, 0	1459	CH_3 deg. deform.
1407 m, —	1409	1394 w, —	1392	νCC + δCH, 19b, B_2
1376 sh, 5p	1376	1377 vw, 6p	1376	CH_3 sym. deform.
1303 m, 0	1307	1288 w, 0	1291	νCC, 14, B_2
1238 s, 20p	1243	1230 vs, 39p	1236	νCO + νCC, 7a′, A_1
1223 vs, —	1224	1215 sh, sh	1219	δCH + νCC, 3, B_2
1204 sh, 8p	1205	1200 m, sh	1202	νCCH_3 + δCH, 7a, A_1
1163 vs, 4p	1170	941 m, —	933	ϕCOH (ϕCOD)
1047 w, 5p	1054	1047 w, 4p	1054	δCH + δCD, 9a, A_1
980 vw, —	978	988 w, —	985	CH_3 rock
872 —, 6p	862	871 sh, 8p	857	δCD, 18a, A_1
867 m, —	881	867 m, —	870	δCD, 15, B_2
815 w, 100p 799 w, 36p ‡	816	813 w, 100p 797 vw, 34p ‡	815	νCCH_3 + νCO + νCC, 1, A_1
715 m, —	710	711 m, —	704	νCCH_3 + νCO, 13, A_1
632 vw, 15dp	637	631 —, 14dp	636	γCCC, 6b, B_2
459 —, 40p	458	456 —, 38p	455	γCCC, 6a, A_1
413 w, —	416	—	401	δCO + δCCH_3, 9b, B_2
330, —, 22dp	329	329 —, 20dp	324	δCCH_3 + δCO, 18b, B_2
Out-of-plane				
1454 sh, —	1458	—	1458	CH_3 deg. deform.
1038 sh, —	1039	1038 sh, —	1039	CH_3 rock
925 w, 0	923	—	923	πCH, 17a, A_2
889 m, 0	890	887 m, —	890	πCH, 5, B_1
729 m, —	729	729 m, —	729	πCD, 11, B_1
705 sh, —	706	—	706	πCD, 10a, A_2
670 vw, 2dp	667	670 vw, 1	667	πCO + τCC, 4, B_1
454 s, —	448	452 s, —	448	πCCH_3 + πCO, 16b, B_1
387 —, 0§	387	—	386	τCC, 16a, A_2
—	310	—	308	πCCH_3 + πCO + τCC, 10b, B_1
—	292	—	218	τCO
—	143	—	139	τCC + πCCH_3 + πCO, 17b, B_1
—	17	—	17	τCCH_3

Table 3. (*Contd.*)

2,3,5,6-d_4		2,3,5,6-d_4-OD		
ν_{obs}*	ν_{calc}	ν_{obs}*	ν_{calc}	Assignment†
In-plane				
1588 m, 4p	1595	1600 m, 3p 1582 m, 4p ‡	1592	νCC, 8a, A_1
1577 m, 2dp	1576	1570 sh, 1	1567	νCC, 8b, B_2
1462 w, —	1461	1459 w, —	1457	CH$_3$ deg. deform.
1439 vs, 0	1437	1436 vs, 0	1434	νCC, 19a, A_1
1376 sh, 4p	1377	1375 vw, 3p	1375	CH$_3$ sym. deform.
1366 m, —	1372	1350 vw, —	1347	νCC, 19b, B_2
1299 m, 0	1289	1287 w, 0	1281	νCC, 14, B_2
1231 m, 19p	1230	1219 s, 27p	1225	νCC + νCO + νCCH$_3$, 7a′, A_1
1187 vs, 11p	1185	893 s, —	903	ϕCOH (ϕCOD)
1122 m, 1p	1123	1121 m, 1p	1123	νCCH$_3$ + νCO + δCD, 7a, A_1
1036 w, 0	1031	1064 sh, —	1059	δCD, 3, B_2
943 w, —	950	951 w, —	954	CH$_3$ rock
878 w, 18p	863	876 —, 18p	859	δCD + γCCC, 18a, A_1
851 —, 7p	846	849 —, 7p	846	δCD, 9a, A_1
814 w, —	807	814 w, —	807	δCD, 15, B_2
793 m, 100p	799	792 w, 100p	797	νCC + νCCH$_3$ + νCO, 1, A_1
693 m, 3p	690	690 w, 2p	686	νCC + νCCH$_3$ + νCO, 13, A_1
626 vw, 21dp	626	625 vw, 16dp	625	γCCC, 6b, B_2
458 sh, 35p	457	454 w, 30p	453	γCCC, 6a, A_1
401 w, —	405	—	391	δCO + δCCH$_3$, 9b, B_2
323 —, 20dp	328	323 —, 16dp	323	δCCH$_3$ + δCO, 18b, B_2
Out-of-plane				
1462 w, —	1458	1459 w, —	1458	CH$_3$ deg. deform.
1036 w, 0	1038	1034 w, —	1038	CH$_3$ rock
—	811	—	811	πCD, 17a, A_2
—	792	—	792	πCD, 5, B_1
705 s, —	703	705 s, —	703	πCD, 11, B_1
653 vw, —	647	653 vw, —	647	πCD, 10a, A_2
601 w, 5dp	604	601, vw, 4dp	604	τCC + πCCH$_3$ + πCO, 4, B_1
427 s, —	427	427 s, —	427	πCO + πCCH$_3$, 16b, B_1
365 —, 0§	356	—	355	τCC, 16a, A_2
—	304	—	304	πCCH$_3$ + πCO + τCC, 10b, B_1
290¶	290	—	218	τCO
—	142	—	138	τCC + πCCH$_3$ + πCO, 17b, B_1
—	17	—	17	τCCH$_3$

---

*Frequencies (in cm^{-1}) followed by i.r. intensities (vs, very strong; s, strong; m, medium; w, weak; vw, very weak, sh, shoulder) and by relative Raman intensities (100 for the strongest band, sh, shoulder) together with polarization properties (p, polarized; dp, depolarized).

†Approximate descriptions of the calculated modes. For ring vibrations, the corresponding vibrational modes of benzene and the symmetry species under C_{2v} symmetry are indicated.

‡Doublet due to Fermi resonance.

§Liquid state value.

‖Data from Ref. [10].

¶Data from Ref. [8].

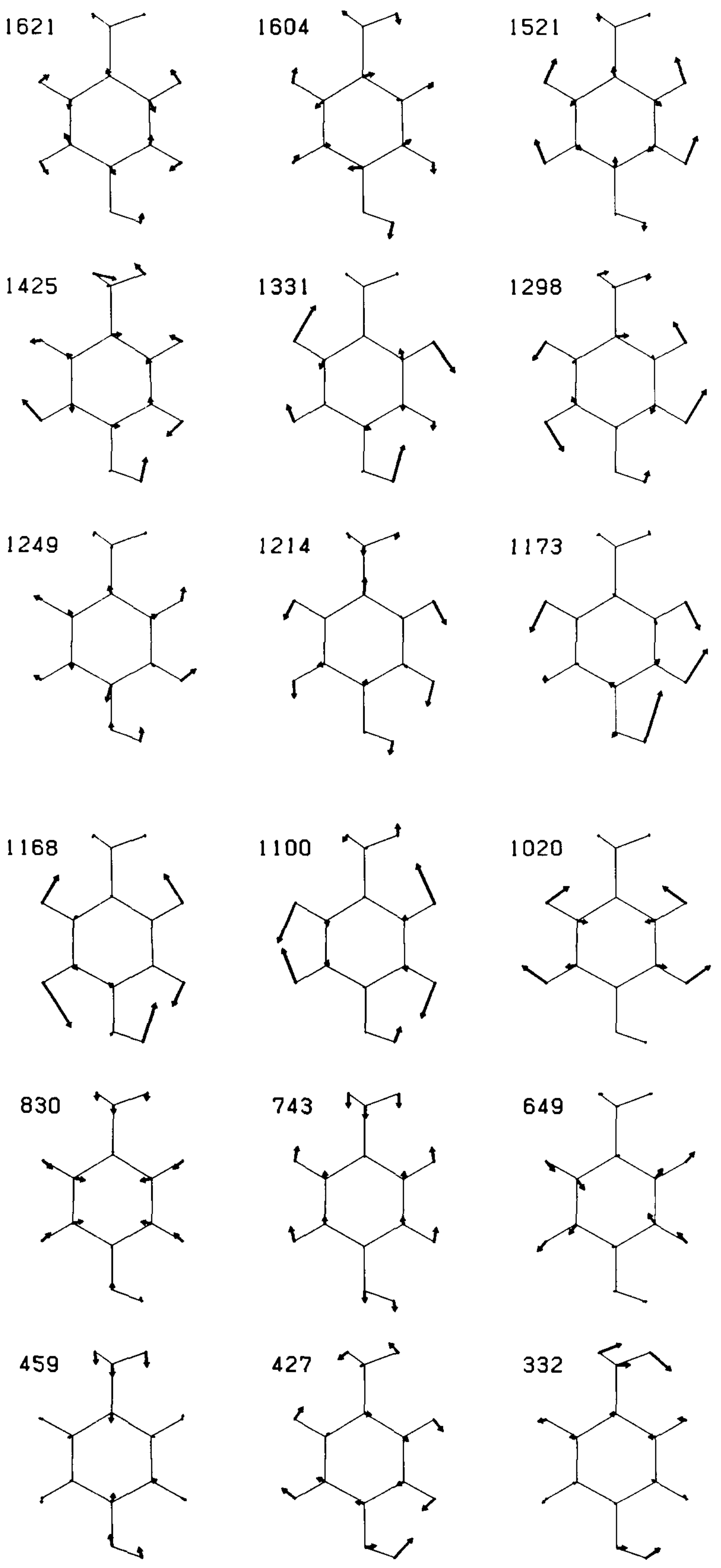

Fig. 7. Normal modes of in-plane vibrations calculated for *p*-cresol-d_0. The displacement vectors are enlarged three times.

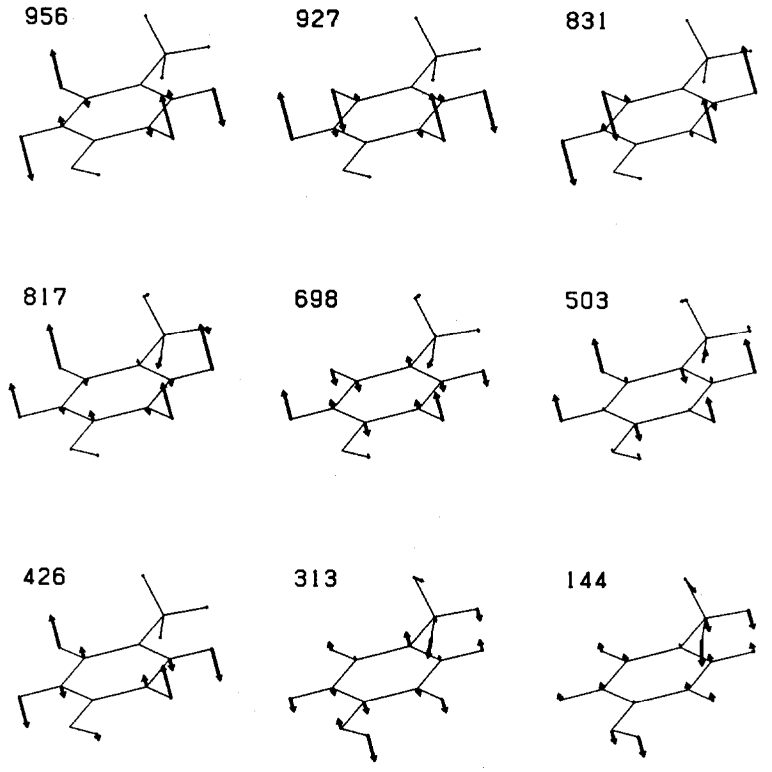

Fig. 8. Normal modes of out-of-plane vibrations calculated for *p*-cresol-d_0. The displacement vectors are enlarged three times.

Table 4. Combination and overtone frequencies of *p*-cresol*

Mode	d_0	2,6-d_2	3,5-d_2	2,3,5,6-d_4
$2\nu_{10a}$	— (1662)	1442 (1442)	— (1410)	1302 (1306)
$\nu_{18a}+\nu_{6b}$	— (1659)	1495 (1491)	1497 (1504)	1498 (1504)
$2\nu_{11}$	1633 (1624)	1501 (1516)	— (1458)	1397 (1410)
$\nu_{13}+\nu_{10a}$	— (1570)	1430 (1427)	1428 (1420)	1338 (1346)
$\nu_{17a}+\nu_{16b}$	— (1452)	— (1377)	1381 (1379)	1240 (1238)
$2\nu_4$	1396 (1400)	1264 (1262)	— (1340)	1210 (1202)
$\nu_5+\nu_{10b}$	1231 (1240)	— (1187)	1195 (1199)	1098 (1096)
$\nu_{11}+\nu_{16a}$	1210 (1226)	1141 (1146)	1124 (1116)	1069 (1070)
$\nu_{13}+\nu_{6a}$	1196 (1200)	— (1166)	1172 (1174)	1151 (1151)
$\nu_{6b}+\nu_{6a}$	1111 (1106)	— (1096)	1100 (1091)	— (1084)
$2\nu_{16b}$	— (1008)	932 (926)	911 (908)	860 (854)
$\nu_{16b}+\nu_{16a}$	— (918)	— (851)	838 (841)	— (792)
$\nu_{16a}+\nu_{10b}$	— (734)	— (694)	696 (697)	— (669)
$\nu_{16a}+2\nu_{17b}$	— (702)	669 (674)	— (673)	631 (649)
$\nu_{16b}+\nu_{17b}$	652 (648)	— (606)	599 (597)	— (569)
$\nu_{18b}+\nu_{17b}$	— (478)	486 (468)	482 (473)	— (465)
$\nu_{10b}+\nu_{17b}$	— (464)	— (449)	443 (453)	446 (446)

*I.r. and Raman frequencies are given in units of cm^{-1}. The frequencies in parentheses are estimated from the fundamental frequencies.

to give key information on the ionization state of the hydroxyl group [23, 24]. As a probe of tyrosine environment, the relative intensity of the 'tyrosine Raman doublet' around 840 cm^{-1} has been found to be useful to distinguish the side chain acting as a proton donor, acceptor or donor–acceptor in hydrogen bonding [22]. This is because the relative intensity of a Fermi doublet is usually sensitive even to a small change in frequency separation between two interacting vibrational levels and such a change can readily be induced by environmental alteration. Similarly, the Fermi doublets newly found here for non-deuterated and deuterated *p*-cresol may be useful in the environmental analysis of tyrosine side chains. Particularly, a strong i.r. doublet observed at 817–804 cm^{-1} for *p*-cresol-d_0 and a strong Raman doublet observed at 815–799 cm^{-1} for *p*-cresol-3,5-d_2 are potential probes. The ν_{8a} Fermi doublets at 1618–1602 cm^{-1} in *p*-cresol-3,5-d_2 and at 1600–1582 cm^{-1} in *p*-cresol-2,3,5,6-d_4-OD may also be useful because the ν_{8a} vibration is very strong in u.v. resonance Raman spectra [4, 6]. In addition, the trio of Raman bands ($\nu_{7a'}$, ν_{7a} and ν_{9a}) in the 1260–1170 cm^{-1} region can be used to monitor the tyrosine environment because the present vibrational analysis suggests that the ϕCOH mode located within this frequency region interacts with the trio and the frequency shift of ϕCOH due to change in the state of the hydrogen bond affects the frequencies and relative intensities of the trio. A change in the intensity pattern of the trio has been found in the u.v. Raman spectra of cytochrome *c* and ascribed to disruption of internal hydrogen bonds of tyrosine side chains [5]. A study of solvent effects on the trio Raman bands is in progress and the results will be reported in a future publication.

CONCLUSION

Assignment of i.r. and Raman bands has been made for eight isotopomers of *p*-cresol. The fundamental frequencies selected from the spectral data are consistently reproduced by normal coordinate calculations. The assignments and calculated normal modes help us to understand the vibrations of tyrosine and to analyse the tyrosine bands in the vibrational spectra of proteins. In particular, several doublet bands due to Fermi resonance and the trio of Raman bands in the 1260–1160 cm^{-1} region are expected to be potential probes for the micro-environments of tyrosine side chains in proteins.

REFERENCES

[1] I. HARADA and H. TAKEUCHI, in *Spectroscopy of Biological Systems, Advances in Spectroscopy*, Vol. 13, pp. 113–175, (Edited by R. J. CLARK and R. E. HESTER). Wiley, Chichester (1986).

[2] R. P. RAVA and T. G. SPIRO, *J. Am. chem. Soc.* **106**, 4062 (1984).

[3] C. R. JOHNSON, M. LUDWIG, S. O'DONNELL and S. A. ASHER, *J. Am. chem. Soc.* **106**, 5008 (1984).

[4] R. P. RAVA and T. G. SPIRO, *J. phys. Chem.* **89**, 1856 (1985).

[5] R. A. COPELAND and T. G. SPIRO, *Biochemistry* **24**, 4960 (1985).

[6] C. R. JOHNSON, M. LUDWIG and S. A. ASHER, *J. Am. chem. Soc.* **108**, 905 (1986); S. A. ASHER, M. LUDWIG and C. R. JOHNSON, *J. Am. chem. Soc.* **108**, 3186 (1986).

[7] H. TAKEUCHI and I. HARADA, *Spectrochim. Acta* **42A**, 1069 (1986).

[8] R. J. JAKOBSEN, *Spectrochim. Acta* **21**, 433 (1965).

[9] N. I. DAVYDOVA, I. A. ZHIGUNOVA, L. A. IGNATYEVA and M. A. KOVNER, *Opt. Spektrosk.* **56**, 1077 (1965); *Opt. Spectrosc., USSR* **18**, 605 (1965).

[10] J. H. S. GREEN, D. J. HARRISON and W. KYNASTON, *Spectrochim. Acta* **27A**, 2199 (1971).

[11] H. R. MATTHEWS, K. S. MATTHEWS and S. J. OPERA, *Biochem. biophys. Acta* **497**, 1 (1977).

[12] M. N. SIAMWIZA, Ph.D. thesis, Massachusetts Institute of Technology, Cambridge, Mass. (1974).

[13] T. SHIMANOUCHI, H. MATSUURA, Y. OGAWA and I. HARADA, *J. phys. Chem. Ref. Data* **7**, 1323 (1978).

[14] C. BOIS, *Acta crystallogr.* **B26**, 2086 (1970).

[15] N. W. LARSEN, *J. molec. Struct.* **51**, 175 (1979).

[16] IUPAC Commission on Molecular Structure and Spectroscopy, *Pure appl. Chem.* **50**, 1707 (1978).

[17] C. LA LAU and R. G. SNYDER, *Spectrochim. Acta* **27A**, 2073 (1971).

[18] H. TAKEUCHI and M. TASUMI, *Chem. Phys.* **77**, 21 (1983).

[19] W. A. KREINER, H. D. RUDOLPH and B. T. TAN, *J. molec. Spectrosc.* **48**, 86 (1973).

[20] N. FUSON, C. CARRIGOU-LAGRANGE and M. L. JOSIEN, *Spectrochim. Acta* **16**, 106 (1960).

[21] K. S. PITZER and D. W. SCOTT, *J. Am. chem. Soc.* **65**, 803 (1943).

[22] M. N. SIAMWIZA, R. C. LORD, M. C. CHEN, T. TAKAMATSU, I. HARADA, H. MATSUURA and T. SHIMANOUCHI, *Biochemistry* **14**, 4870 (1975).

[23] K. J. ROTHSCHILD, R. ROEPE, P. L. AHL, T. N. EARNEST, R. A. BAGOMOLNI, S. K. DAS GUPTA, C. M. MULLIKEN and J. HERZFELD, *Proc. natn. Acad. Sci. U.S.A.* **83**, 347 (1986).

[24] G. DOLLINGER, L. EISENSTEIN, S.-L. LIN, K. NAKANISHI and J. TERMINI, *Biochemistry* **25**, 6524 (1986).